# Two-Dimensional Carbon Incorporation into Si(001): C Amount and Structure of Si(001)-$c(4 \times 4)$

Hanchul Kim,[1] Wondong Kim,[1] Geunseop Lee,[2] and Ja-Yong Koo[1]

[1]*Korea Research Institute of Standards and Science, P.O. Box 102, Yuseong, Daejeon 305-600, Korea*

[2]*Department of Physics, Inha University, Inchon 402-751, Korea*

(Received 13 October 2004; published 22 February 2005)

The C amount and the structure of the Si(001)-$c(4 \times 4)$ surface is studied using scanning tunneling microscopy (STM) and *ab initio* calculations. The $c(4 \times 4)$ phase is found to contain 1/8 monolayer C (1 C atom in each primitive unit cell). From the C amount and the symmetry of high-resolution STM images, it is inferred that the C atoms substitute the fourth-layer site below the dimer row. We construct a structure model relying on *ab initio* energetics and STM simulations. Each C atom induces an on-site dimer vacancy and two adjacent rotated dimers on the same dimer row. The $c(4 \times 4)$ phase constitutes the subsurface $Si_{0.875}C_{0.125}$ $\delta$ layer with two-dimensionally ordered C atoms.

DOI: 10.1103/PhysRevLett.94.076102 PACS numbers: 68.37.Ef, 68.35.Dv, 68.35.Md, 68.55.Ln

Carbon incorporation into Si(001) is important in developing noble technologies compatible with the silicon technology. To list several of many, they are high-speed Si-based devices, strain engineering, band gap tailoring, and surface functionalization. Such developments are generally prevented from the extremely low solubility ($\lesssim 10^{-3}\%$) of C in bulk Si. But, there have been some reports that C atoms can be incorporated into Si(001) up to a few tens of percent using nonequilibrium methods [1–3]. This enhanced near-surface solubility was ascribed to the energy lowering through the coupling of the impurity stress to the surface stress field [2].

A microscopic understanding on the initial C incorporation into Si(001) was achieved only very recently [4]. In the isolated incorporation, C atoms adopt a very stable configuration, the so-called DV41 defect shown in Fig. 1(a). Such DV41 defects arrange into one-dimensional (1D) line segments across the dimer rows at low C concentrations, forming a $2 \times n$ superstructure. With more C atoms, it has been observed that patches of a two-dimensional (2D) $c(4 \times 4)$ phase are formed [5].

The Si(001)-$c(4 \times 4)$ phase has been extensively studied for several decades, but no consensus has been reached yet on its atomic structure. It has been reported to be formed by various procedures: Si homoepitaxy [6,7], exposure to various gases such as $H_2$ [8,9], $Si_2H_6$ [10], $C_2H_2$ [11], and $C_2H_4$ [12], adsorption and desorption of Bi [13] or S [14], and even the simple annealing of Si(001) in ultrahigh vacuum (UHV) [15,16]. Early studies claimed that the $c(4 \times 4)$ phase is one of the intrinsic Si(001) reconstructions without any foreign element [8,14]. Such a claim has been rebutted by recent studies, and the existence of C is generally accepted [9,12,15–19]. However, it is still under debate as to the role of C in forming Si(001)-$c(4 \times 4)$. Some claim that C atoms provide global strain inducing the $c(4 \times 4)$ reconstruction of Si(001) [15,17]. Others consider C to be a basic ingredient of the $c(4 \times 4)$ phase [9,12,18,19]. Accordingly, several structural models have been proposed with [9,12,16,18] or without [8,17] C atoms [see Figs. 1(b)–1(e)]. In this sense, the C concentration is at the center of the debate, but it is still controversial despite several attempts to measure it [15–17].

In this Letter, we report a comprehensive study using scanning tunneling microscopy (STM) on the C-incorporated Si(001) surface. Two phases, the $2 \times n$ and the $c(4 \times 4)$, coexist for the C concentration between 0.05 and 0.12 monolayer (ML). [We define 1 ML as the C concentration equivalent to 1 C atom per $1 \times 1$ unit cell of Si(001).] By analyzing the STM images, the C concentration in the $c(4 \times 4)$ phase is found to be 1/8 ML. We propose models of the $c(4 \times 4)$ phase which are compatible with the C amount and the symmetry of the STM images and examine them by *ab initio* total energy calculations and STM image simulations. The models are characterized by the DV41 defect and two adjacent 90°-rotated Si dimers (RDs).

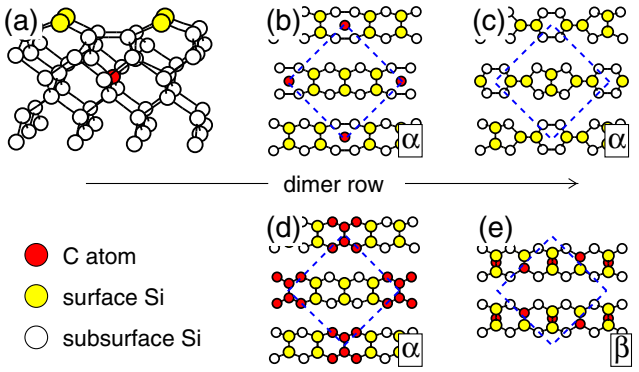


FIG. 1 (color online). (a) A bird's eye view of the C-induced DV41 defect. (b)–(e) Schematic diagrams of previously proposed models for the Si(001)-$c(4 \times 4)$ phase: (b) missing dimer [16], (c) ad-dimer [8], (d) six-C-cluster [9,18], and (e) Si-C heterodimer [12] models. Atoms in two surface layers and the fourth-layer C [(b),(e)] are shown. Dashed squares indicate the $\sqrt{8} \times \sqrt{8}$-$R45°$ primitive unit cell.

 © 2005 The American Physical Society

Experiments were performed using a homemade STM in an UHV chamber with the base pressure of $1.2 \times 10^{-10}$ Torr [20]. We used $C_2H_2$ gas as the C source, since the $C_2H_2$ molecules chemisorb uniformly on the Si(001) surface with the probability near unity at room temperature (RT) [21], and the chemisorbed molecules are effectively dissociated by brief heating [22]. The $C_2H_2$ gas was dosed on the Si(001) surface at RT by backfilling the UHV chamber at $6.2 \times 10^{-10}$ Torr. Subsequent annealing of the sample at 900–1000 K for 2 min causes thermal dissociation of $C_2H_2$ and C incorporation into Si(001).

The concentration of incorporated C atoms ($\theta_C$) was determined from the dosing time and then calibrated to the number of DV41 defects counted in the samples having only the $2 \times n$ phase. Notice that the number of C atoms in the $2 \times n$ phase can be measured unambiguously by counting DV41 defects. In our experiments, dosing time as long as 24 s was needed to increase 0.01 ML of C concentration. This makes the experimental procedure stable and controllable. The error in the C concentration is estimated to be smaller than 0.005 ML.

We have performed an extensive set of STM experiments by varying $\theta_C$. For $\theta_C$ below 0.05 ML, we observed only one type of C-induced STM feature, which is the DV41 defect [4]. At around $\theta_C = 0.05$ ML, the $c(4 \times 4)$ phase begins to appear as small patches. The $c(4 \times 4)$ patches grow with increasing $\theta_C$ and cover the whole surface at around 0.12 ML [see Figs. 2(a)–2(c)]. For the $\theta_C$ above 0.13 ML, the surface develops roughness, and we could not obtain atomically flat terraces. It is likely that the C concentration in the $c(4 \times 4)$ phase, $\theta_{c(4\times4)}$, is 1/8 ML, implying *one* C atom incorporated in each primitive unit cell on the average. This may support the picture that C is a constituent of the $c(4 \times 4)$ phase.

For a more quantitative analysis, we examined the lower coverage regime where the $c(4 \times 4)$ and the $2 \times n$ phases coexist. We prepared several tens of C-incorporated Si(001) surfaces by varying $\theta_C$ in the range between 0.06 and 0.12 ML. For these samples, we measured the fractional area ($S$) of the $c(4 \times 4)$ phase using STM images of an area as large as $1500 \times 1500$ Å$^2$ to guarantee the statistical analysis. Figure 3 shows a plot of the measured $S$ versus $\theta_C$. The linear regression analysis yields $S = a\theta_C + b$ with $a = 14.00 \pm 0.58$ and $b = -0.70 \pm 0.05$. Considering the conservation of incorporated C atoms that can be expressed by

$$\theta_C = S\theta_{c(4\times4)} + (1 - S)\theta_{2\times n}; \qquad S = \frac{\theta_C - \theta_{2\times n}}{\theta_{c(4\times4)} - \theta_{2\times n}},$$

where $\theta_{2\times n}$ is the C concentration in the coexisting $2 \times n$ phase, the linear regression results are translated into $\theta_{c(4\times4)} = 0.12 \pm 0.01$ and $\theta_{2\times n} = 0.05 \pm 0.006$ ML. This estimate of $\theta_{c(4\times4)}$ agrees with the implication from the fully covered $c(4 \times 4)$ phase and leads us to conclude that $\theta_{c(4\times4)} = 1/8$ ML regardless of $\theta_C$.

To verify the validity of the above procedure, we performed independent measurements of $\theta_{2\times n}$. For $\theta_C$ ranging from 0.07 to 0.09 ML, where the $2 \times n$ patches are large enough to guarantee the negligible statistical error, we measured $\theta_{2\times n}$ by counting the DV41 defect in the $2 \times n$ regions of the STM images. The measured $\theta_{2\times n}$ was $0.048 \pm 0.004$ ML regardless of $\theta_C$, agreeing with the estimate from the linear regression analysis.

Now we describe the characteristics of the $c(4 \times 4)$ phase that should be satisfied by any plausible structure model. From the high-resolution STM images such as the insets of Fig. 2, four experimental constraints can be extracted. (i) There exist two different primitive cells, called $\alpha$ and $\beta$, with random distribution and approximately equal population. (ii) In the filled-state image [Fig. 2(c)], the $\alpha$ cell shows a bright oblong protrusion which has been thought to be the normal Si dimer [9,16,17]. Then the central depression in the $\beta$ cell is believed to be the dimer vacancy (DV). (iii) Within both $\alpha$ and $\beta$ cells, the STM image appears symmetric with respect to both the dimer-bond and the dimer-row directions. (iv) Regardless of $\alpha$ or $\beta$, pairs of round protrusions are formed on and directed along dimer rows with $\times 4$

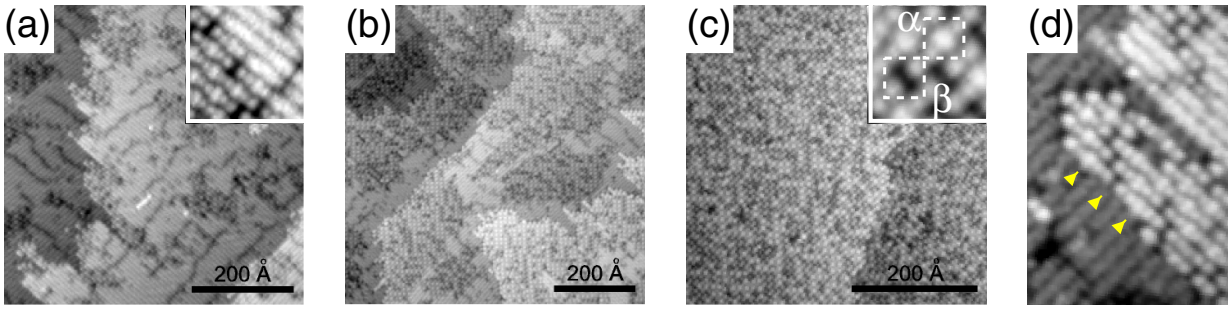


FIG. 2 (color online). Filled-state STM images of C-incorporated Si(001) with different C concentrations ($\theta_C$). (a) $\theta_C \simeq 0.06$ ML, where the $c(4 \times 4)$ patches are surrounded by the $2 \times n$ phase. The inset shows that the $c(4 \times 4)$ phase appears darker than the $2 \times n$ phase on the same terrace. (b) $\theta_C \simeq 0.11$ ML, where the $c(4 \times 4)$ phase is the majority. (c) $\theta_C \simeq 0.12$ ML, where the whole surface is covered with the $c(4 \times 4)$ phase. The inset shows both $\alpha$ and $\beta$ primitive unit cells of the $c(4 \times 4)$ phase. (d) A two-terrace image clearly showing that the central features (a bright protrusion in the $\alpha$ cell and a depression in the $\beta$ cell) of upper-terrace $c(4 \times 4)$ cells are in registry with every second dimer row on the lower terrace, as pointed out by the arrowheads, indicating the $\times 4$ periodicity.

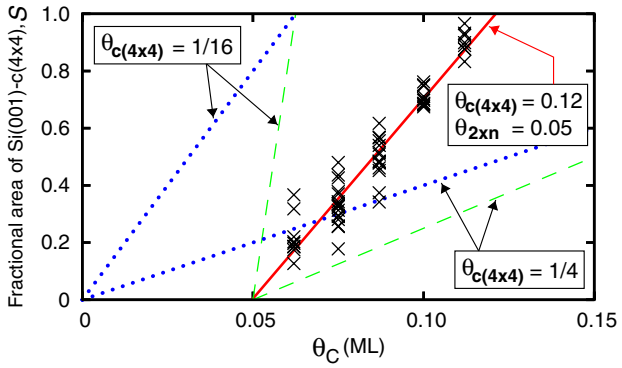


FIG. 3 (color online). The fractional area ($S$) occupied by the $c(4 \times 4)$ phase at different $\theta_C$'s. The symbols ( $\times$ ) are measured data and the thick solid line is the linear fit. Dashed (dotted) lines are hypothetical curves for $\theta_{c(4\times4)} = 1/16$ and $1/4$ with $\theta_{2\times n} = 0.05$ (0.0) ML.

periodicity as seen in the inset of Fig. 2(a) and in Fig. 2(d). The paired round protrusions are 180° out of phase on neighboring dimer rows and complete the perfect $c(4 \times 4)$ order [see the corners of the dashed squares in Fig. 2(c)].

Let us test previously proposed models of Si(001)-$c(4 \times 4)$ on the ground of the aforementioned constraints. Of the previous models shown in Figs. 1(b)–1(e), the ad-dimer and six-C-cluster models satisfy constraints (i)–(iv) but contradict our finding of $\theta_{c(4\times4)} = 1/8$ ML. The Si-C heterodimer model [12] incorrectly predicts the pairing of round protrusions across the dimer rows, contradicting constraint (iv). In addition, it contains 1/4 ML C, being incompatible with the present C amount result. Hence the models of Figs. 1(c)–1(e) should be excluded. The missing dimer model in Fig. 1(b) is compatible with all the constraints and the C amount and is examined by *ab initio* calculations as described below.

The C amount of $\theta_{c(4\times4)} = 1/8$ ML can be realized in many ways. The simplest case would be the structures with uniform C distribution, i.e., with 1 C atom in each $\sqrt{8} \times \sqrt{8}$-$R45°$ cell. Or, one can imagine structures with 0 and 2 C atoms in two adjacent $\sqrt{8} \times \sqrt{8}$-$R45°$ cells. Finally, many structures with even less uniform C distribution can be devised.

Restricted to the simplest case, due to constraints (iii) and (iv), C atoms should occupy the fourth-layer site under the dimer row. This inferred C site is compatible with a recent photoemission spectroscopy study suggesting the presence of the unique subsurface C species [19]. The C atom incorporated in this site is known to create a DV above it and to form the DV41 defect [4]. Thus we construct models based on the DV41 defects. The simplest model is the DV41$_\alpha$ shown in Fig. 4(a), which is constructed by placing DV41 defects with the $c(4 \times 4)$ periodicity. This model turns out to be the same as the previously proposed missing dimer model [Fig. 1(b)]. The model DV41$_\beta$ for the $\beta$ cell is derived from DV41$_\alpha$ by removing the Si dimer in between two DV41s. We obtain the

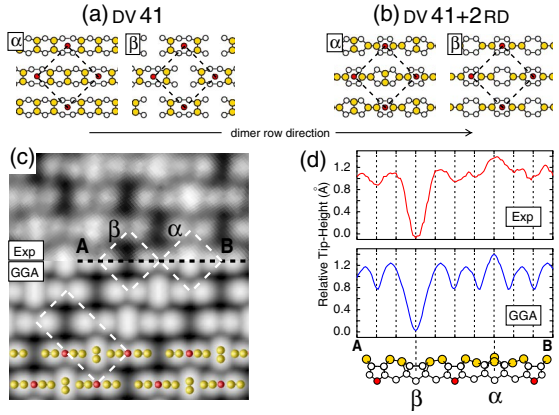


FIG. 4 (color online). Schematic diagrams of the models based on (a) DV41 and (b) DV41 + 2RD. (c),(d) STM simulations on the RD$_{\alpha\beta}$ model are compared with experiments at the sample bias voltage of $-2.5$ V: (c) the filled-state STM image and (d) the line profile along $\overline{AB}$ in (c) with the side view of RD$_{\alpha\beta}$. The dashed squares and rectangle indicate $\sqrt{8} \times \sqrt{8}$-$R45°$ and $2\sqrt{8} \times \sqrt{8}$-$R45°$ primitive unit cells, respectively.

other set of models, (DV41 + 2RD)$_\alpha$ and (DV41 + 2RD)$_\beta$ shown in Fig. 4(b), by rotating the Si dimers adjacent to the DV41 defect in DV41$_\alpha$ and DV41$_\beta$ by 90°, respectively. We call these models RD$_\alpha$ and RD$_\beta$ for simplicity.

We examined the proposed models by performing the density-functional theory (DFT) calculations within the generalized gradient approximation using the VASP [23] and ultrasoft pseudopotentials [24]. We used the energy cutoff of 300 eV and the $k$ points equivalent to an $8 \times 8$ mesh within the $1 \times 1$ surface Brillouin zone. The theoretical lattice constant was 5.46 Å. The surface was modeled by a slab composed of ten Si layers with a H passivated bottom surface and an 8-Å-thick vacuum. The $c(4 \times 4)$ conventional unit cell was used, unless stated otherwise. We optimized the geometries until the forces on atoms became smaller than 0.01 eV/Å while the H atoms and the two bottom Si layers are fixed.

The stability of the proposed models was examined by calculating the surface free energy $F(\nu)$ of the model $\nu$,

$$F(\nu) \equiv E_{\mathrm{DFT}}(\nu) - n_{\mathrm{Si}}(\nu)\mu_{\mathrm{Si}} - n_{\mathrm{C}}(\nu)\mu_{\mathrm{C}},$$

where $E_{\mathrm{DFT}}$ is the DFT total energy, $n_X$ and $\mu_X$ are the number of atoms and the chemical potential for atomic type $X$ ($X$ = Si or C), respectively [25]. The RD$_\alpha$ and RD$_\beta$ are found to be energetically comparable, showing the energy difference as small as 0.04 eV/($\sqrt{8} \times \sqrt{8}$). On the other hand, the DV41$_\alpha$ and DV41$_\beta$ are energetically unfavored by 0.11 and 0.77 eV/($\sqrt{8} \times \sqrt{8}$), respectively, compared with the RD$_\alpha$. This suggests that the DV41$_\alpha$ and DV41$_\beta$ models may be excluded.

Then, to simulate the experimental observation (i) of coexisting $\alpha$ and $\beta$ cells, we examined a structure with the mixed pair of the $\alpha$ and $\beta$ cells aligned along the dimer row, using a $2\sqrt{8} \times \sqrt{8}$-$R45°$ surface cell. This structure is

designated as $RD_{\alpha\beta}$ and is shown in Figs. 4(c) and 4(d). The $RD_{\alpha\beta}$ is found to be more stable than the $RD_\alpha$ by 0.06 eV/$(\sqrt{8}\times\sqrt{8})$. This may explain the observation that the $\alpha$ and $\beta$ cells are almost equally populated. Using the relaxed geometry, the constant-current STM images were calculated within the Tersoff-Hamann approximation [26]. The theoretical STM image and the line profile of $RD_{\alpha\beta}$ reproduce the experimental feature well, as compared in Figs. 4(c) and 4(d) [27,28].

For the cases of less uniform C distribution, we considered a model with two alternating $\sqrt{8}\times\sqrt{8}$-$R45°$ cells where one cell contains *two* C atoms at the third-layer sites (the DV32 configuration in Ref. [4]) and the other *none*. This model turns out to have higher energy than the $RD_{\alpha\beta}$ by 1.0 eV/$(\sqrt{8}\times\sqrt{8})$. Based on this, we infer that structures with more localized C atoms (or less uniform C distribution) should have even higher energy. This, in conjunction with the energetics and STM simulations for the uniform C distribution, suggests that the $RD_\alpha$ and $RD_\beta$ models are the structures for the $\alpha$ and $\beta$ cells of Si(001)-$c(4\times4)$, respectively.

According to our models, the paired round protrusions are identified as two buckled RDs next to the DV41 defect. To elucidate the origin of dimer rotation, we examined a *lower coverage* (1/16 ML) case employing $2\times8$ structures with C-induced defects running across the dimer rows, where C atoms are arranged in $\times8$ periodicity along the dimer row. The $2\times8$ structure with DV41 defects, which is in fact the lowest energy configuration at this coverage [4], is calculated to be more stable than that with (DV41 + 2RD) defects by 0.12 eV/(C atom). This stability is opposed to the 1/8-ML $c(4\times4)$ case, where the $RD_\alpha$ model is more stable than the $DV41_\alpha$ by 0.11 eV/(C atom). Thus, the dimer rotation in the $c(4\times4)$ phase seems to occur to relieve the increased tensile stress due to the $\times4$ arranged C atoms along the dimer row.

It is interesting to notice that C atoms adopt a unique structural and chemical configuration in various C-containing phases. In the isolated incorporation, the DV41 defect is formed. By increasing the C amount, the DV41s form segments of chains, and finally the $c(4\times4)$ reconstruction. However, the surface structures are differently modified to relieve the stress effectively for different C amounts. The resulting Si(001) surfaces provide the subsurface $Si_{1-x}C_x$ $\delta$ layers with either 1D $(2\times n)$ or 2D $[c(4\times4)]$ ordering of C atoms. Thus the C incorporation into Si(001) can be utilized for the strain engineering of Si-based devices or for the controlled growth of various nanostructures.

In conclusion, we have determined the C amount in the C-incorporated Si(001)-$c(4\times4)$ surface using STM. On the average, the $c(4\times4)$ phase contains 1/8 ML C. We constructed structure models of the $c(4\times4)$ phase, which contains *one* C atom *in each* $\sqrt{8}\times\sqrt{8}$-$R45°$ cell. The models are characterized by the DV41 defect and two adjacent RDs. *Ab initio* calculations show that the proposed models are energetically favorable and reproduce the STM features well.

This work is supported by Ministry of Science and Technology of Korea through "The Creative Research Initiative" and "The National R&D Project for Nano Science and Technology." H. K. acknowledges support from the KISTI under "The Fifth Strategic Supercomputing Support Program."

[1] H. Rucker, M. Methfessel, E. Bugiel, and H. J. Osten, Phys. Rev. Lett. **72**, 3578 (1994).
[2] J. Tersoff, Phys. Rev. Lett. **74**, 5080 (1995).
[3] K. Brunner, K. Eberl, and W. Winter, Phys. Rev. Lett. **76**, 303 (1996), and references therein.
[4] W. Kim, H. Kim, G. Lee, and J.-Y. Koo, Phys. Rev. Lett. **89**, 106102 (2002).
[5] W. Kim *et al.*, Surf. Sci. **516**, L553 (2002).
[6] R. N. Thomas and M. H. Francombe, Appl. Phys. Lett. **11**, 108 (1967).
[7] T. Sakamoto *et al.*, Surf. Sci. **86**, 102 (1979).
[8] R. I. G. Uhrberg *et al.*, Phys. Rev. B **46**, 10 251 (1992).
[9] J. Y. Maeng and S. Kim, Surf. Sci. **482–485**, 1445 (2001).
[10] W. K. Liu *et al.*, Surf. Sci. **264**, 301 (1992).
[11] L. Li *et al.*, Phys. Rev. B **56**, 4648 (1997).
[12] L. Simon *et al.*, Phys. Rev. B **64**, 035306 (2001).
[13] A. Goryachko *et al.*, Surf. Sci. **497**, 47 (2002).
[14] P. Moriarty, L. Koenders, and G. Hughes, Phys. Rev. B **47**, 15 950 (1993).
[15] K. Miki, K. Sakamoto, and T. Sakamoto, Appl. Phys. Lett. **71**, 3266 (1997).
[16] H. Nörenberg and G. A. D. Briggs, Surf. Sci. **430**, 154 (1999).
[17] S. T. Jemander, H. M. Zhang, R. I. G. Uhrberg, and G. V. Hansson, Phys. Rev. B **65**, 115321 (2002).
[18] O. Leifeld *et al.*, Phys. Rev. Lett. **82**, 972 (1999).
[19] J. R. Ahn, H. S. Lee, Y. K. Kim, and H.-W. Yeom, Phys. Rev. B **69**, 233306 (2004).
[20] J.-Y. Koo *et al.*, Phys. Rev. B **57**, 8782 (1998).
[21] W. Kim *et al.*, Phys. Rev. B **64**, 193313 (2001).
[22] P. A. Taylor *et al.*, J. Am. Chem. Soc. **114**, 6754 (1992); C. Huang, W. Widdra, X. S. Wang, and W. H. Weinberg, J. Vac. Sci. Technol. A **11**, 2250 (1993).
[23] G. Kresse and J. Furthmüller, Phys. Rev. B **54**, 11 169 (1996).
[24] D. Vanderbilt, Phys. Rev. B **41**, R7892 (1990).
[25] We used the cohesive energy of bulk Si for $\mu_{Si}$, which is usual. Regardless of the choice of $\mu_C$, the relative stability is not affected since the number of C atoms is the same in all the considered models.
[26] J. Tersoff and D. R. Hamann, Phys. Rev. Lett. **50**, 1998 (1983); Phys. Rev. B **31**, 805 (1985).
[27] In contrast to normal Si dimers, RDs would not undergo flip-flop motion at RT as the environment of two atoms in a RD are inequivalent. The RDs buckled in the other way were unstable and relaxed back to the configuration as shown in Fig. 4.
[28] Simulations with DV41-based models show poor agreement with the experimental images.